THE JOURNAL OF PHYSICAL CHEMISTRY C

Article

pubs.acs.org/JPCC

Heterochiral Domain Formation in Homochiral α-Dipalmitoylphosphatidylcholine (DPPC) Langmuir Monolayers at the Air/Water Interface

Lu Lin,[†,‡] Anan Liu,[†,‡] and Yuan Guo*[,†]

[†]Beijing National Laboratory of Molecular Sciences, State Key Laboratory of Molecular Reaction Dynamics, Institute of Chemistry, and [‡]Graduate University, Chinese Academy of Sciences, Beijing 100190, China

ABSTRACT: α-Dipalmitoylphosphatidylcholine (DPPC) Langmuir monolayers at the air/water interface are an important biomimetic system. Previous studies using optical imaging have shown that enantiomerically pure DPPC molecules form periodical homochiral domains with close packing. However, it is unclear whether the chirality of these domains is stable or dynamic. Recently, we investigated the chirality of L-DPPC Langmuir monolayers using second-harmonic-generation linear dichroism (SHG-LD). The change in the degree of chiral excess (DCE) and its sign with time indicated that the chirality transformed from homochiral to heterochiral domains, with an associated change in handedness. Here we propose that hydrolysis of L-DPPC is responsible for the formation of the opposite chiral state. On the basis of quantum chemistry calculations and effective pair potential (EPP) theory, we give a molecular explanation for this transformation. These results provide an insight into the lipid monolayers that the chiral state of domains composed of chiral lipids is dynamic.

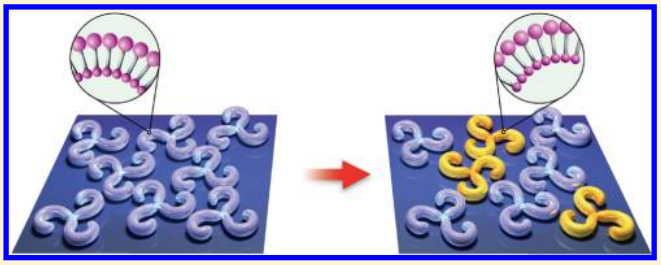

INTRODUCTION

Lipid monolayers and bilayers receive a great deal of attention because of their important biological role as a principle component of biological membranes. Nowadays, these lipid layers are used as simple model systems to investigate the physicochemical properties of biological membranes.[1] These systems are known to be self-aggregating and are driven by hydrophobic effects and headgroup interactions between the lipid molecules, resulting in mesoscopic domain structures with a variety of morphologies. The sizes and shapes of the domains are also important because the lipid molecules play a functional biological role in the form of various assemblies.[2,3] For example, most of the molecules comprising the cell membrane, such as phospholipids, are chiral, and in many cases this chirality has a major influence on the domain shapes and patterns of the self-aggregated systems. These chiral molecules act as building blocks and are likely to form macromolecule chiral assemblies in lipid monolayers and bilayers, which is referred to as structural or orientational chirality.[4,5] Specific chiral structures could play an important role in determining the relative position of transmembrane proteins and in controlling the functionality of transmembrane proteins that act as an efficient receptor or part of the membrane channel.[6] Consequently, any variation in these chiral structures may lead to a change in functionality of the molecules. This poses the question: do the dynamics of the lipid monolayer and bilayer affect the structural chirality of domains within the lipid monolayer and bilayer themselves? In other words, is the structural chirality of the assemblies static or dynamic?

It is generally accepted that the lipid bilayer is dynamic in biological membrane, having four possible mobility models of fast lateral diffusion, phospholipid flip-flop, intrachain motion of fatty acyl, and fast axial rotation within the bilayer structure.[6] Although there has been considerable interest in lipid mobility, such as phospholipid flip-flop,[7−15] there have been few studies on the dynamics of the structural chirality in lipid monolayers and bilayers.

α-Dipalmitoylphosphatidylcholine (DPPC) Langmuir monolayers at the air/water interface are important biomimetic membrane systems and have been widely studied using surface pressure−area (π−A) isotherms, fluorescence microscopy,[16] Brewster angle microscopy (BAM),[17,18] and Maxwell displacement current (MDC).[18] Surface pressure isotherms of the Langmuir monolayers at the air/water interface suggest that DPPC molecules undergo a phase transition with increasing the surface pressure when the monolayers is compressed.[16] Periodic clover-type domains are observed using florescence microscopy and BAM in the liquid-condensed phase region. DPPC is a chiral amphiphilic molecule with one chiral center. The domain of DPPC assemblies has a macromolecule chiral structure with the curvature related to the chirality of DPPC. L-DPPC and D-DPPC molecules form chiral domains, whereas racemic DPPC mixtures form achiral domains with noncurved arms.[19] Previous work focused only on the observation of DPPC domains, whereas few studies reported the stability and

Received: November 16, 2011
Revised: June 14, 2012
Published: June 19, 2012

dynamics of the chirality of these domains. In this work, we have applied second-harmonic-generation linear dichroism (SHG-LD) to detect the chirality of L-DPPC Langmuir monolayers and have investigated the transformation of the chirality of L-DPPC domains with time.

SHG-LD is a nonlinear optical method that is specific and sensitive not only to surface structure but also to chirality. This property is based on the fact that second-order nonlinear optical processes are dipole-forbidden in centrosymmetric media.[20,21] Hence, SHG-LD is inherently suitable for characterizing the interfacial chirality, especially for weakly chiral interfaces.[22]

When a laser beam with frequency ω is incident onto the interface, an optical signal with frequency 2ω can be detected in the direction of the reflection. In SHG-LD, the incident light is linearly polarized. The SHG intensity is proportional to the square of the mode of the effective second-order susceptibility of the interface, as expressed in eq 1.

$$I(2\omega) = \frac{32\pi^3\omega^2\sec^2\beta}{c_0^3 n_1^2(\omega)n_1(2\omega)}|\chi_{\text{eff}}^{(2)}|^2 I^2(\omega) \tag{1}$$

where $n_1(\omega)$ and $n_1(2\omega)$ are the refractive indices of phase 1 at frequencies ω and 2ω, respectively, and β is the incident angle. The effective second-order susceptibility, $\chi_{\text{eff}}^{(2)}$, is related to the macroscopic second-order susceptibility tensor, $\chi_{ijk}^{(2)}$, as expressed in eq 2

$$\chi_{\text{eff}}^{(2)} = [L(2\omega)\colon \vec{e}(2\omega)]\cdot\chi_{ijk}^{(2)}\colon [L(\omega)\colon \vec{e}(\omega)]\cdot[L(\omega)\colon \vec{e}(\omega)] \tag{2}$$

where $L(\omega_i)$ is the local field factor tensor and $\vec{e}(\omega_i)$ is the unit vector of the corresponding optical field. The macroscopic second-order susceptibility $\chi_{ijk}^{(2)}$ is a third-rank tensor with 27 elements, which can be reduced to several nonzero independent elements according to the symmetry of the interface. For isotropic chiral interfaces, there are four nonzero independent tensor elements, χ_{zzz}, $\chi_{zxx} = \chi_{zyy}$, $\chi_{xzx} = \chi_{xxz} = \chi_{yzy} = \chi_{yyz}$, and $\chi_{xyz} = \chi_{xzy} = -\chi_{yzx} = -\chi_{yxz}$. Of the four elements, only the last one (χ_{xyz}) is related to the interfacial chirality, named χ_{chiral}, and the other tensor elements are achiral.

For rotationally isotropic chiral interfaces, the effective second-order susceptibility can be expressed as

$$\begin{aligned}\chi_{\text{eff},\alpha_{\text{in}}-\gamma_{\text{out}}} &= [\chi_{\text{eff,45s}}\sin 2\alpha + \chi_{\text{eff,chiral}}\cos^2\alpha]\sin\gamma \\ &\quad + [\chi_{\text{eff},sp}\sin^2\alpha + \chi_{\text{eff},pp}\cos^2\alpha + \chi_{\text{eff,chiral}} \\ &\quad \sin\alpha\cos\alpha]\cos\gamma\end{aligned} \tag{3}$$

with

$$\begin{aligned}\chi_{\text{eff,sp}} &= L_{zz}(2\omega)L_{yy}(\omega)L_{yy}(\omega)\sin\beta\chi_{zyy} \\ \chi_{\text{eff,45s}} &= L_{yy}(2\omega)L_{zz}(\omega)L_{yy}(\omega)\sin\beta\chi_{yzy} \\ \chi_{\text{eff,pp}} &= -2L_{xx}(2\omega)L_{zz}(\omega)L_{xx}(\omega)\cos^2\beta \\ &\quad \sin\beta\chi_{xzx} \\ &\quad + L_{zz}(2\omega)L_{xx}(\omega)L_{xx}(\omega) \\ &\quad \sin\beta\cos^2\beta\chi_{zxx} \\ &\quad + L_{zz}(2\omega)L_{zz}(\omega)L_{zz}(\omega)\sin^3\beta\chi_{zzz} \\ \chi_{\text{eff,chiral}} &= 2L_{xx}(2\omega)L_{yy}(\omega)L_{zz}(\omega)\sin\beta\cos\beta\chi_{xyz}\end{aligned} \tag{4}$$

where α is the incident polarization angle and γ is the output polarization angle. The subscript p denotes polarization within the plane of the incident beam and the surface normal, and s denotes polarization parallel to the interface. In our experiments, the detection polarization is fixed to s, called s-detection, because we have proven that s-detection is simpler and more accurate than p-detection in the SHG-LD method.[23] For s-detection, $\gamma = \pi/2$ and the SHG intensity can be expressed as

$$I_s \propto |\chi_{\text{eff,45s}}\sin 2\alpha + \chi_{\text{eff,chiral}}\cos^2\alpha|^2 \tag{5}$$

In the present work, we have confirmed that the L-DPPC monolayer is chiral, which is in agreement with previous results of BAM experiments.[17,18] In addition, we also observed the transformation of the chiral states of the L-DPPC monolayer with time, which indicates that the structural chirality of the L-DPPC domains is likely to be dynamic in the lipid monolayer.

EXPERIMENT

L-DPPC was purchased from Sigma-Aldrich and was used without further purification. Chloroform solution (0.5 mM) was used for spreading. We spread 50 μL on the pure water subphase (Millipore, 18.2 MΩ·cm) in a Teflon trough with an area of 80 cm^2, and on average one molecule occupied 0.53 nm^2, corresponding to the liquid-condensed phase region of the surface pressure isotherm. Before detection, the solvent was allowed to evaporate from the air/water interface for more than 15 min to allow the L-DPPC molecules forming the monolayer and the monolayer to achieve thermodynamic equilibrium by means of free diffusion and intermolecular interactions. The surface pressure was measured using a normalized commercial pressure sensor (PS4, Nima) on each day.

The SHG-LD experimental setup was similar to that previously reported.[23,24] A mode-locked femtosecond Ti/sapphire laser (Tsunami 3960C, Spectra-Physics) with a repetition rate of 82 MHz and a pulse width of 80 fs was used for the SHG-LD measurements. The laser beam was focused onto the interface using a lens with a 10 cm focal length. The incident light wavelength was 800 nm, and the incident angle was 70° with a typical laser power of 600 mW. The incident polarization angle was adjusted using a rotating half-wave plate driven by a computer-controlled stepper motor. SHG signals were collected with a high-gain photomultiplier tube (Hamamatsu) and single photon counting system (SR400, Stanford Research Systems) at different incident polarization angles. The supporting stage below the trough could be translated, and we chose several positions of the monolayer to detect the SHG-LD signal. In this way, we were able to obtain dependence curves of the relationship between SHG intensity

dx.doi.org/10.1021/jp2110314 | J. Phys. Chem. C 2012, 116, 14863−14872

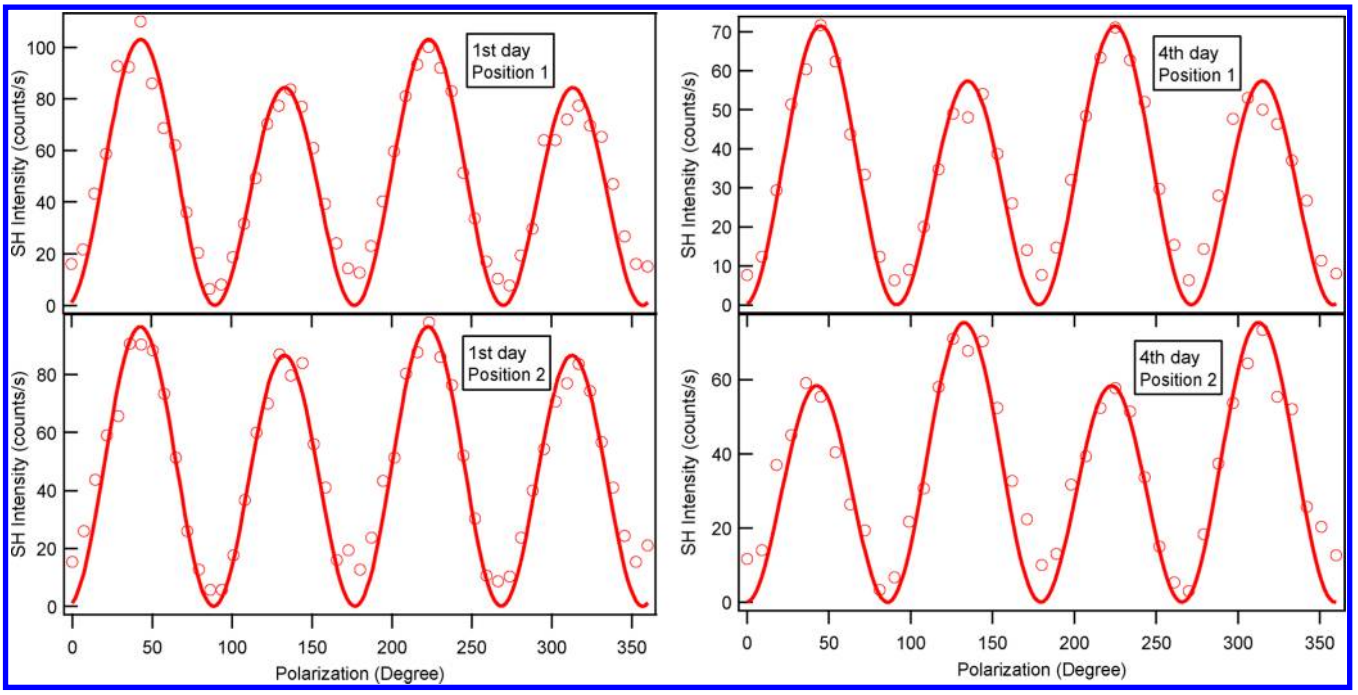

Figure 1. Dependence curves of SHG intensity versus the incident polarization angle for L-DPPC fitted using eq 5. The circles indicate the experimental values and the solid curves are the fitted results. The two curves on the left correspond to positions of the L-DPPC monolayer on the first day, whereas the two on the right were recorded on the fourth day.

and the incident polarization angle for different positions of the monolayer and at different times.

For comparison, we also performed SHG-LD experiments on pure water, racemic DPPC Langmuir monolayers on pure water subphase, and L-DPPC monolayers on NaOH aqueous solution subphase. Racemic DPPC and sodium hydroxide were purchased from Sigma-Aldrich and used without further purification. The Langmuir monolayers were prepared in the same way as those of L-DPPC monolayers on pure water subphase. The pH of NaOH aqueous solution was 12.6. We then chose several positions to carry out the SHG-LD measurements.

RESULTS AND DISCUSSION

The surface pressure on each day is 13.9, 16.8, 10.4, and 8.3 mN/m, respectively, indicating that the interfacial structure varied gradually. We will discuss this in detail at the end of this section.

We applied the concept of the degree of chiral excess (DCE) to describe the interfacial chirality quantitatively.[22,23] DCE is defined as

$$\Delta I/I = \frac{2(I_{-45^\circ} - I_{+45^\circ})}{(I_{-45^\circ} + I_{-45^\circ})} \quad (6)$$

where I_{-45° and I_{+45° are the SHG intensity with incident laser polarization of $-45^\circ(135^\circ)$ and $+45^\circ$, respectively. The physical meaning of DCE can be interpreted as: for achiral interfaces, $\chi_{chiral} = 0$, leading to $I_{-45^\circ} = I_{+45^\circ}$ and DCE = 0; for chiral interfaces, $\chi_{chiral} \neq 0$ and DCE $\neq$ 0. In SHG-LD experiments for detecting the chirality of monolayers, it is generally recognized that the chiral signal originates from the structural chirality (orientational chirality), together with the mesoscopic helical structures of some curvatures.[4,5] The curvature of the helix determines the absolute value of DCE. A greater curvature results in a greater DCE value. Opposite helical directions give rise to opposite signs of DCE, so the sign of DCE indicates whether the chiral interface is predominantly in one chiral enantiomer state or the opposite chiral enantiomer state. In other words, the value and sign of DCE gives a quantitative description of the state of the interfacial chirality.

Figure 1 shows the difference in SHG intensities of L-DPPC in the range of incident polarization angles from I_{+45° to I_{-45°. The difference indicates that the monolayer is chiral, according to the definition of DCE above. In contrast, no chiral signal was detected for pure water subphase and racemic DPPC monolayers (Figures 2 and 3), where the SHG intensities are almost equal when the incident polarization angle is I_{+45° and I_{-45°. The achirality of the pure water subphase indicates that the chiral signal originates from the L-DPPC monolayer, whereas racemic DPPC monolayers are known to be achiral, and this proves the reliability of the detection method.

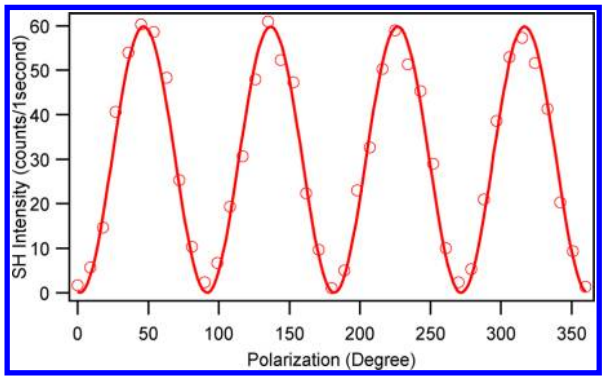

Figure 2. Dependence curves of the SHG intensity versus the incident polarization angle for pure water subphase fitted using eq 5. The circles indicate experimental values and the solid curve is the fitted result.

dx.doi.org/10.1021/jp2110314 | J. Phys. Chem. C 2012, 116, 14863−14872

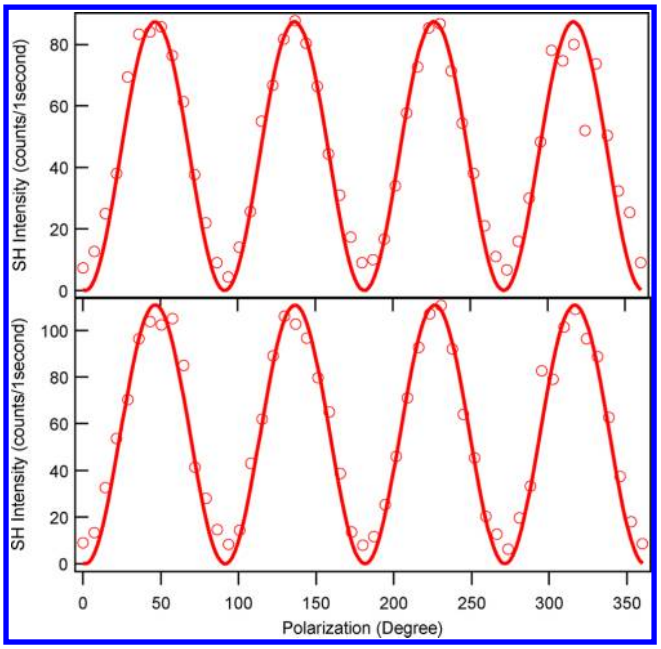

Figure 3. Dependence curves of the SHG intensity versus the incident polarization angle for racemic DPPC monolayers at two different positions fitted using eq 5. The circles indicate experimental values and the solid curves are the fitted results.

However, the differences between the SHG signals (Figure 1) do not necessarily indicate that the L-DPPC monolayer is chiral because in-plane anisotropy also brings about similar differences in SHG-LD experiments.[23] This is called false chirality. For this reason, the differences in Figure 1 may arise from either interfacial or false chirality. That is, false chirality may interfere with the detection of the interfacial chirality by the SHG-LD method. To confirm that Figure 1 does indeed reflect the true chirality of the L-DPPC monolayer, the possibility of false chirality must be ruled out. In the following section, we will estimate of the SHG signal that arises from false chirality.

The anisotropy of the interface can be classified into two categories according to the symmetry.[22] For an interface with C_{1h} and C_{3v} symmetry, the s-in/s-out signal should be nonzero.[23] This signal was not present in any of the SHG results obtained from our experiments (Figure 1). Therefore, the possibility of false chirality of C_{1h} and C_{3v} symmetry can be ruled out. For an interface with C_{2v} symmetry, the signal is complex. In our previous work, we introduced the ratio $\delta_{\chi_{eff,45s}}/\delta_{\chi_{eff,chiral}}$ for different positions to determine if the surface is with in-plane C_{2v} anisotropy or without. The ratio is expected to be a constant of $1/(2\cos\beta)$.[23] Here δ indicates the variation at different positions. If the differences between the SHG signals were caused by the in-plane C_{2v} symmetry, then the ratio $\delta_{\chi_{eff,45s}}/\delta_{\chi_{eff,chiral}}$ for different positions would be $1/(2\cos 70^\circ) = 1.46$ for our experimental configuration. Table 1 lists the fitting results of $\chi_{eff,45s}$ and $\chi_{eff,chiral}$ for several adjacent positions of the monolayer. It shows that the variation of $\chi_{eff,chiral}$ and $\chi_{eff,45s}$ for different detecting position is different; $\chi_{eff,chiral}$ varies greatly, whereas $\chi_{eff,45s}$ remains almost constant. Therefore, $\delta_{\chi_{eff,45s}}/\delta_{\chi_{eff,chiral}} \ll 1$, ruling out the possibility of C_{2v} symmetry. Hence, we regard the SHG intensities between the incident polarization angles of I_{+45° and I_{-45° as chiral signals and the monolayers as chiral, in accordance with previous results.[16−18]

Table 1. Fitting Results of $\chi_{eff,45s}$ and $\chi_{eff,chiral}$ for Different Positions Recorded on the Fourth Day

$\chi_{eff,45s}$	$\chi_{eff,chiral}$	DCE
7.3 ± 0.1	0.92 ± 0.10	0.25 ± 0.03
7.3 ± 0.2	0.60 ± 0.22	0.16 ± 0.06
7.4 ± 0.1	−1.1 ± 0.2	−0.30 ± 0.04
7.4 ± 0.1	0.56 ± 0.14	0.15 ± 0.04
7.4 ± 0.1	1.1 ± 0.1	0.29 ± 0.04
7.6 ± 0.2	−0.47 ± 0.16	−0.12 ± 0.04
7.5 ± 0.1	0.97 ± 0.15	0.26 ± 0.05
7.4 ± 0.1	−0.29 ± 0.12	−0.079 ± 0.030

To confirm our experimental reliability of the heterochiral domain formation in homochiral DPPC monolayer, we performed several sets of experiments. For most of our experiments, the results of the heterochiral domain formation in the homochiral DPPC monolayer have good reproducibility. Figure 4 gives the results of two sets, which shows a

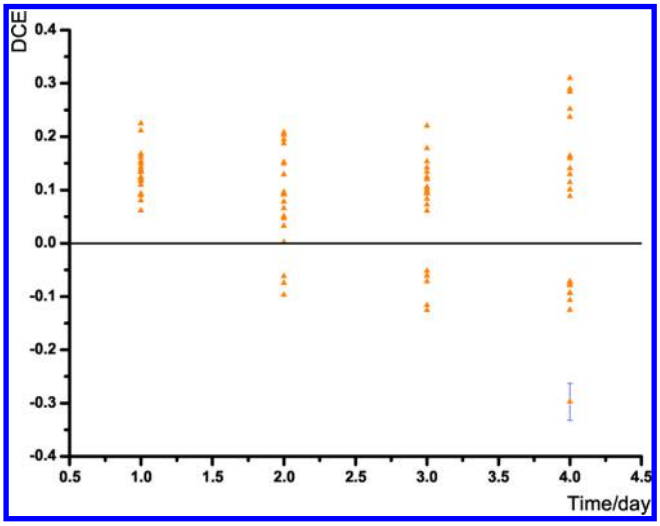

Figure 4. DCE of each position plotted against day after spreading. Experimental results of two sets are integrated. In sets 1 and 2, eight and twelve positions were recorded on each day, respectively. The solid line is $\Delta I/I = 0$, indicating the achiral state. The nonzero value of DCE indicates that the interface is chiral. The different sign of DCE on the second, third, and fourth days indicates two chiral enantiomer states.

quantitative comparison of the chirality of each position at different times calculated by DCE and indicates the spatial and temporal distributions of the chirality in the L-DPPC monolayer. It can be seen that all of the DCE values in Figure 4 are nonzero, which indicates that the L-DPPC Langmuir monolayer is chiral. All DCE values are positive on the first day, indicating that the morphologies in the L-DPPC monolayers lie in identical chiral states with the same handedness. We refer to mesoscopic structures with identical chiral states as homochiral domains. However, the DCE values are not equal, indicating that the degree of the chirality is not the same at all positions. These results reveal that helical morphologies with the same helical direction and different values of curvature are formed in the process of L-DPPC aggregating at the air/water interface. Careful analysis of the DCE values in Figure 4 reveals an important fact that the sign of the DCE is not the same for all positions on the second, third, and fourth days. Because opposite signs represent different chiral enantiomer states, it

dx.doi.org/10.1021/jp2110314 | J. Phys. Chem. C 2012, 116, 14863−14872

can be inferred that mesoscopic structures with different chiral states exist in the L-DPPC monolayer on the second, third, and fourth day. In other words, morphologies with opposite helical directions are formed given a sufficient length of time. Mesoscopic structures with different chiral states are referred to as heterochiral domains. This observation indicates that macroscopic chirality of L-DPPC is changeable in the time scale of a few days. Moreover, that the chirality of the L-DPPC monolayer is dynamic on this time scale.

To our knowledge, there has previously been no theoretical and experimental evidence to suggest that domains of enantiomerically pure L-DPPC molecules can change chirality. It is necessary to elucidate the nature of the conversion at the molecular level. In the following section, we will give an explanation of this chiral transformation using quantum chemistry and effective pair potential (EPP) theory. We will mainly focus on the mechanism of formation for new domains with opposite chirality.

At the beginning of this study, we assumed that the L-DPPC monolayer was in a nonequilibrium state and that the molecules could aggregate to form domains with either one chiral state or the mirror image state at different positions. Then, after period of time, the systems reached their thermodynamic equilibrium state and the L-DPPC molecules organized into mesoscopic structures. As a result, there should be only domains with identical chiral enantiomer state in the monolayer. However, we have observed domains with an opposite chiral state on the second, third, and fourth days. In other words, after a long enough time the L-DPPC molecules can organize into mesoscopic structures with a different conformation, and new domains with an opposite chiral state can gradually form. Because the newly formed domains cannot be composed of L-DPPC molecules, there must be new species in the monolayer.

Macroscopic chiral assemblies are composed of basic units called chiral blocks. In the process of chiral transformation, we propose that L-DPPC molecules serve as one type of chiral block to make up the chiral domains, whereas a new species serves as another type and forms chiral domains with an opposite chiral state. The coexistence of L-DPPC molecules and new chiral blocks offers the possibility of chiral transformation in the L-DPPC monolayer. It has been reported that both oxidation and hydrolysis occur in the phospholipid monolayer.[25−29] The products from these reactions could serve as new chiral blocks for constructing domains with a different chirality.

The first possibility for producing new species is that the oxidation of L-DPPC produces new species. Investigation of the oxidation of the phospholipid monolayer has shown that unsaturated phospholipids are easily oxidized at C=C bond sites, whereas phospholipids with fully saturated aliphatic chains, such as L-DPPC, cannot be oxidized.[25−28] In addition, a study of the reaction between gas-phase ozone and monolayers of 1-palmitoyl-2-oleoyl-*sn*-glycero-3-phosphocholine (POPC) has indicated that the headgroup remains almost unchanged during the reaction.[27] Because the headgroup of L-DPPC is the same as that of POPC, we can conclude that the headgroups were not oxidized during our experiments. Hence, the possibility of oxidation can be ruled out.

The other possibility for producing new species is the hydrolysis of L-DPPC to hydrolyzate. Investigation of the hydrolysis of DPPC using differential scanning calorimetric analysis has shown that spontaneous hydrolysis can take place, although the rate is slow.[29] Slow spontaneous hydrolysis of L-DPPC would not provide sufficient hydrolyzate to form opposite chiral domains at the beginning of our experiment. However, with the accumulation of hydrolyzate, new domains with an opposite chiral state could be gradually constructed. Therefore, no opposite chiral signals with negative DCE would be detected at the beginning of our experiments, but as the hydrolysis products gradually formed, the possibility of detecting opposite chiral signals would increase. This was the case with our results. The L-DPPC hydrolyzate could then serve as a new chiral block to fabricate new chiral domains with an opposite chiral state to the L-DPPC chiral domains.

To confirm further the molecular mechanism of switching surface chirality by the hydrolysis, we performed SHG-LD experiments of L-DPPC monolayer on NaOH aqueous solution subphase. The results are shown in Figure 5. For L-DPPC monolayers on pure water subphase, no opposite chiral state could be observed on the first day. However, in the case of NaOH aqueous solution subphase (pH 12.6), transformation of the chiral state could be detected 6 h after spreading of the monolayer. Because the hydrolysis rate is dependent on the pH, we attribute the rapid transformation to the catalysis of hydrolysis by a higher pH. This experiment provides indirect evidence of the proposed molecular mechanism. In the following, we will discuss this mechanism in terms of molecular theory.

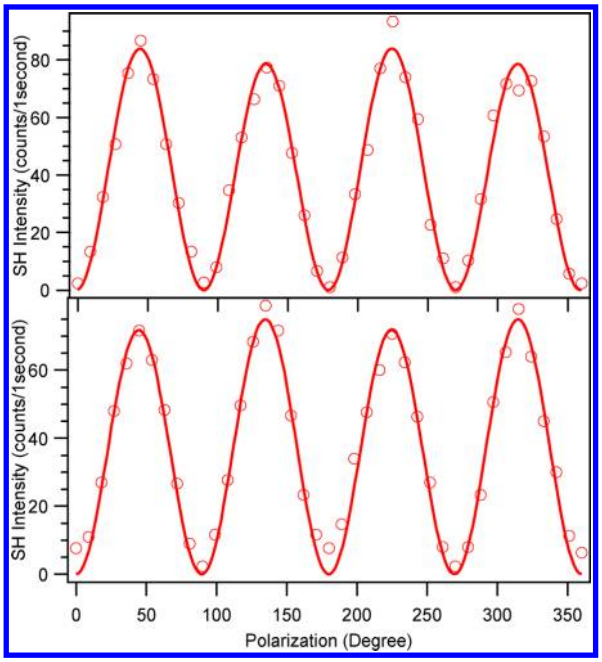

Figure 5. Dependence curves of SHG intensity versus the incident polarization angle for L-DPPC monolayer on NaOH aqueous solution subphase fitted using eq 5. The circles indicate the experimental values, and the solid curves are the fitted results. The two curves correspond to two positions with opposite chiral states. The results were recorded 6 h after spreading of the monolayer.

It has been reported that the L-DPPC molecule has four possible hydrolysis sites, which are shown in Chart 1 and labeled as A_1, A_2, C, and D.[30] To ascertain which site of hydrolysis would lead to the transformation of chiral states, we first investigated the possibility of hydrolysis at each site using quantum chemical methods. The structure of L-DPPC was fully optimized at the UHF/6-31G(d) level of theory. A natural bond orbital (NBO) population analysis[31] was then performed

dx.doi.org/10.1021/jp2110314 | J. Phys. Chem. C 2012, 116, 14863−14872

Chart 1. Molecular Structure of L-DPPC and the Four Possible Hydrolysis Sites Labeled A_1, A_2, C, and D

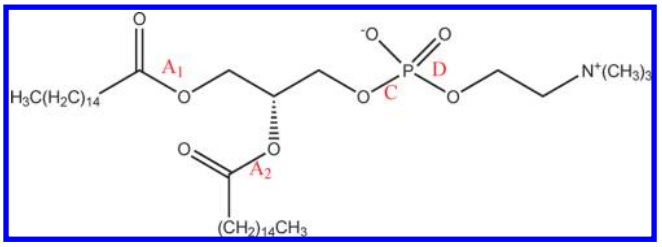

based on the UHF/6-31G(d) optimized geometry to obtain the molecular frontier orbital properties and the natural charge distribution, giving the bond orders thst relate to the possibility of hydrolysis. The calculations were performed using the Gaussian 03 software package.[32]

The bond orders at hydrolysis site A_1, A_2, C, and D were calculated as 0.99636, 0.99620, 0.98805, and 0.98798, respectively, which indicates that each site has almost the same likelihood of hydrolysis. That is, hydrolysis is possible at all four sites, and the four hydrolyzates produced by the hydrolysis could serve as chiral building blocks for constructing chiral domains. However, the hydrolysis site responsible for the construction of the opposite chiral domains was still unclear.

Using molecular theory of helical structures from single chiral molecules, we propose a molecular interpretation of the chiral transformation. A number of continuum and molecular theories have been proposed for the mechanism of chiral structure formation by chiral amphiphilic molecules.[33−39] Among these, the EPP theory proposed by Nandi and Bagchi[39] is simple, and the predictions based on EPP theory are in good agreement with experimental results.[39−41] Here EPP theory is used to analyze which hydrolysis mode dominates the transformation of chiral states.

According to EPP theory, chiral amphiphilic molecules can form chiral structures and patterns at the air/water interface if the monolayer is closely packed and there are strong interactions between the molecules. In the case of L-DPPC (Figure 6), the four groups attached to the chiral center are

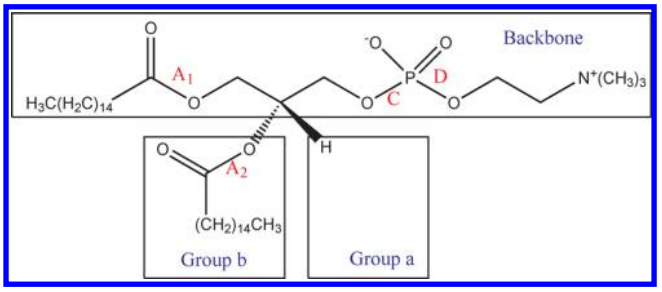

Figure 6. Structure of L-DPPC. The headgroup and the larger hydrophobic chain make up the backbone. The other hydrophobic chain is group b, and the H atom is group a. Hydrolysis sites C, D, and A_1 are contained in the backbone, whereas site A_2 is in group b.

composed of two hydrophobic chains, one hydrophilic headgroup, and one hydrogen atom. The headgroup b′ and the longer chain t, which contains the A_1 hydrolysis site, make up the backbone of the molecule. The sizes of the other two groups determine the characteristics of the molecular aggregation, that is, the chirality of the domains. For convenience, we label the smaller group (H atom) as group a and the other group as group b.

We calculated the EPP profiles for each pair of chiral blocks using the method proposed by Nandi and Bagchi. All parameters were calculated based on the data and formula provided by Bondi[42] and Benamotz and Herschbach.[43] The calculated results are shown in Table 2 and Figures 7−9. σ_a and

Table 2. EPP calculated results

amphiphile	σ_a/angstrom	σ_b/angstrom	Φ_M/deg
L-DPPC	1.4	8.35	45
C	1.4	8.35	45
D	1.4	8.35	45
A_2	1.4	1.92	15
A_1	1.4	3.49	36

σ_b are the diameters of groups a and group b. r is the distance between the centers of two adjacent molecules. U is the EPP. Φ_M is the twist angle between two molecules. In Table 2, the calculated Φ_M denotes the twist angle when the EPP between two molecules is a minimum. This can also be seen in Figures 7−9. The nonzero values of Φ_M indicate that these chiral blocks can form helical structures in a close packed arrangement so as to reduce the EPP. However, the helical direction of each pair of amphiphiles remains unclear. Further analysis is required on the aggregation behavior of these chiral blocks.

To understand which mode of hydrolysis causes the change of chiral states, we need to compare the aggregation behavior of the hydrolyzate with that of L-DPPC. We first consider the hydrolysis sites C and D in the headgroup (Figure 10). If hydrolysis occurs at site C or D, the hydrolyzate will have a different headgroup than L-DPPC, but the groups a and b will be unchanged. Consequently, the aggregation behavior of the hydrolyzate will be similar to that of L-DPPC. When amphiphiles C (or D) join, the helix formed will have the same helical direction as that formed of L-DPPC molecules. Furthermore, the twist angle between a pair of amphiphiles C (or D) will be that the same as for a pair of L-DPPC molecules. Therefore, the new domain formed by the hydrolyzates formed by hydrolysis at site C (or D) will have the same chiral state as the L-DPPC.

Next, we will consider the hydrolysis at site A_2, which is in group b (Figure 11). The backbone remains unchanged by hydrolysis, whereas group b changes to a hydroxyl group, which is still larger than H atom. On the basis of EPP theory, where the characteristics of aggregation are determined by the sizes of groups a and b, we can conclude that the A_2 hydrolyzate will aggregate in a similar way to L-DPPC. Even though the twist angle between a pair of A_2 hydrolyzate is different from that of a pair of L-DPPC molecules according to the EPP calculations, the helical directions of these two pairs will be the same, as will the chiral state and the sign of DCE.

Finally, hydrolysis at site A_1 is considered (Figure 12). A_1 is located in the longer chain t, which is part of the molecular backbone. After hydrolysis at the A_1 site, the original backbone is destroyed, with the headgroup and the hydrophobic chain containing A_2 becoming the new backbone. As a consequence, the hydrolyzate formed by hydrolysis of L-DPPC at site A_1 has a larger group b and a smaller group a. Group a is now an H atom, located opposite to where it is located in L-DPPC molecule with respect to the chiral center (Figure 6), resulting in inverse aggregation behavior. The helical direction between a pair of hydrolyzate A_1 molecules is opposite to that of a pair of L-DPPC molecules, as shown in Figure 13, giving a different

dx.doi.org/10.1021/jp2110314 | J. Phys. Chem. C 2012, 116, 14863−14872

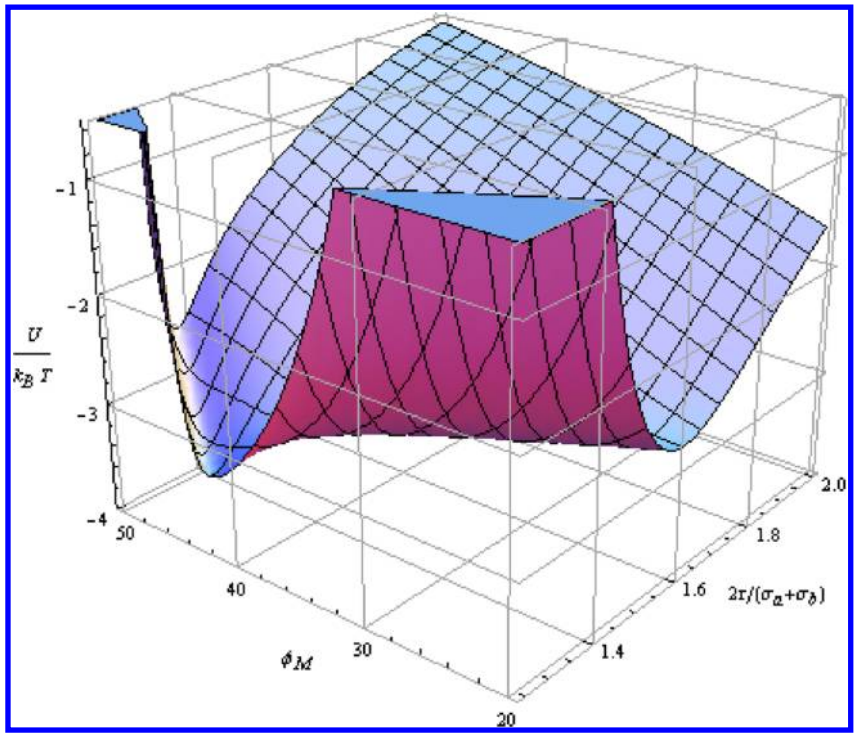

Figure 7. Calculated effective pair potential contour for a pair of L-DPPC molecules. The potential is plotted against the twist angle and the separation between the chiral centers. The diameters of groups a and b are 1.4 and 8.35 Å, respectively. For amphiphiles C and D, the profiles are the same as that of L-DPPC because groups a and b remain unchanged if hydrolysis takes place at site C or D.

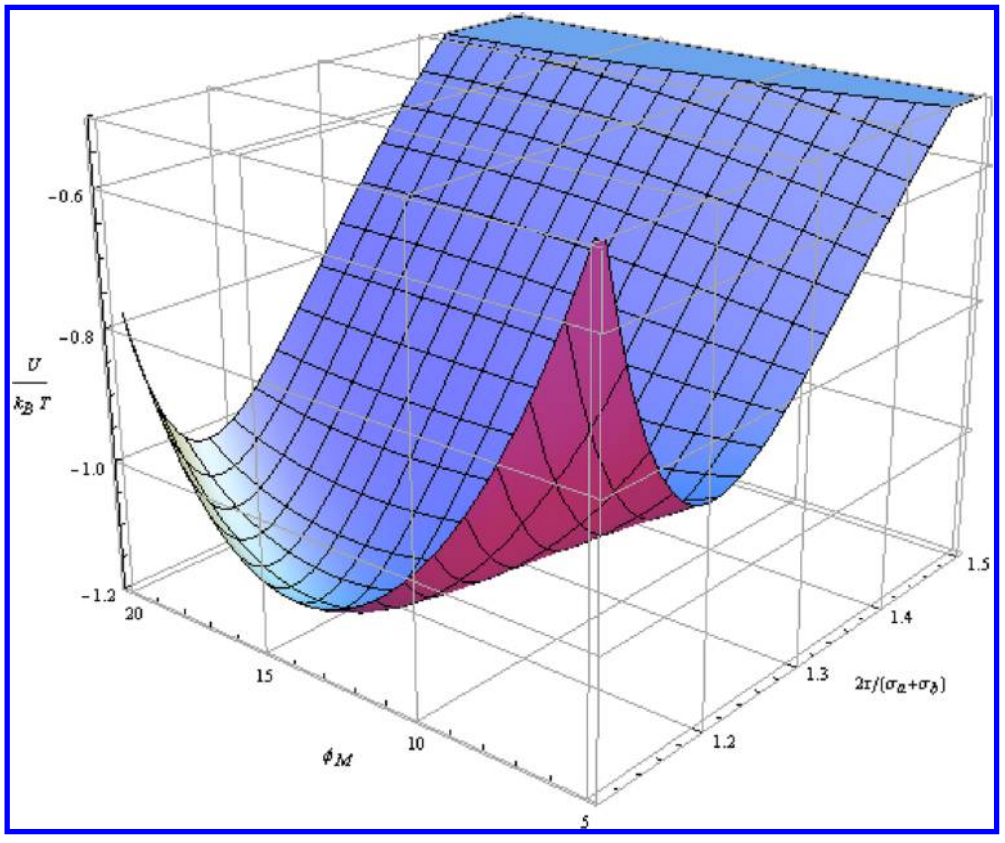

Figure 8. Calculated effective pair potential contour for a pair of amphiphile A_2 molecules. The potential is plotted against the twist angle and the separation between the chiral centers. The diameters of groups a and b are 1.4 and 1.92 Å, respectively.

chiral state. Hence, hydrolysis at A_1 caused the change in chirality of the L-DPPC Langmuir monolayer.

The evolution of the surface pressure can also serve as an indirect evidence of this conclusion. The surface pressure first

dx.doi.org/10.1021/jp2110314 | J. Phys. Chem. C 2012, 116, 14863−14872

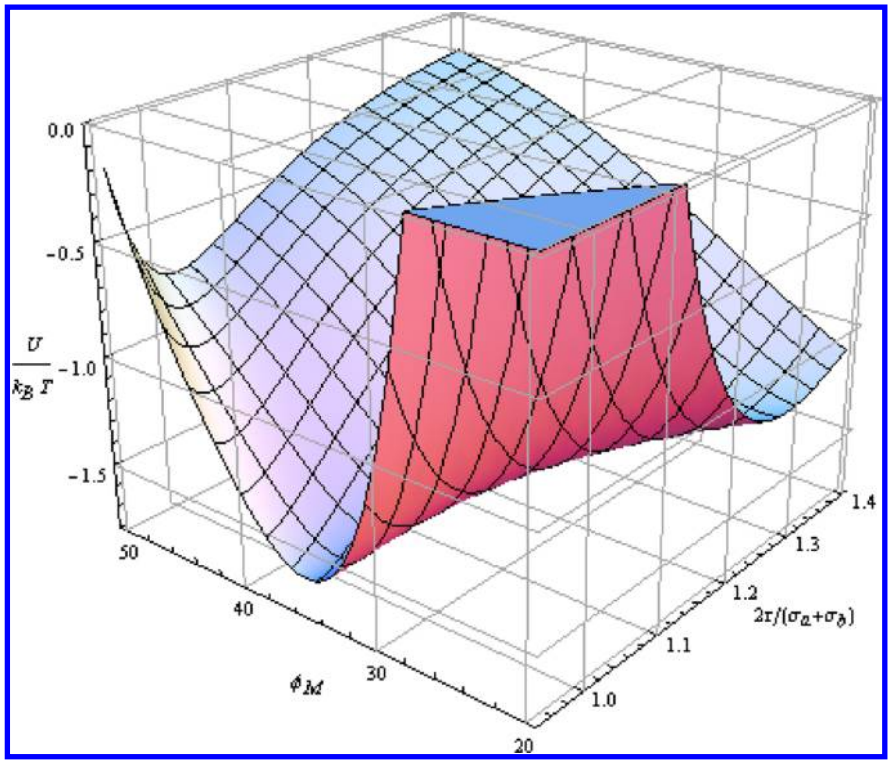

Figure 9. Calculated effective pair potential contour for a pair of amphiphile A_1 molecules. The potential is plotted against the twist angle and the separation between the chiral centers. The diameters of groups a and b are 1.4 and 3.49 Å, respectively.

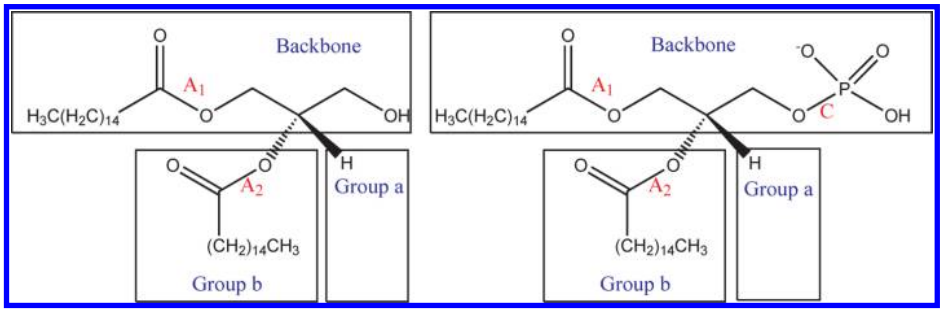

Figure 10. Structures of hydrolyzate formed by hydrolysis at sites C (left) and D (right). C and D are contained in the headgroup. These two hydrolysis products have the same groups a and b as L-DPPC. Therefore, aggregation of a pair of amphiphile C or a pair of amphiphile D is similar to that of a pair of L-DPPC molecules.

increased and then decreased greatly. We attribute the increase in the surface pressure to the hydrolysis, which caused an increase in the molecular density. However, with the accumulation of the hydrolysis products, domains with different sizes, patterns, and chiral states gradually formed, making the monolayer less ordered than at the beginning. As a result, the surface pressure decreased. Moreover, some of the hydrolysis products may be water-soluble, resulting in a decrease in the molecular density and the surface pressure.

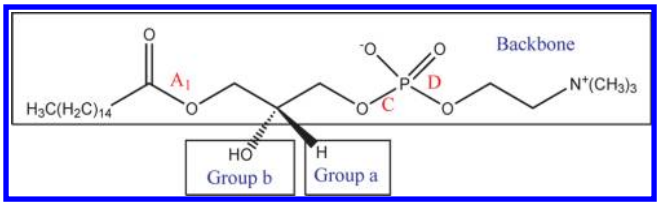

Figure 11. Structure of hydrolyzate formed by hydrolysis at site A_2 in group b. Amphiphile A_2 has the same backbone but a smaller group b than L-DPPC. As a result, the twist angle Φ_M between a pair of amphiphiles A_2 is less than that of L-DPPC. The relative locations of groups a and b with respect to the chiral centers are the same in amphiphile A_2 and L-DPPC, as are the helical directions between a pair of amphiphile A_2 molecules and a pair of L-DPPC molecules.

CONCLUSIONS

Chirality of the L-α-dipalmitoylphosphatidylcholine Langmuir monolayer has been investigated by SHG-LD. We observed a transformation from homochiral domains to heterochiral domains in the L-DPPC monolayer that had not been seen before. This indicated that the domains in L-DPPC Langmuir monolayers could change their chirality given a long enough time. We proposed that the hydrolysis of L-DPPC molecules led to the transformation. EPP theory was used to analyze the aggregation behavior of the hydrolyzates formed by hydrolysis at the four possible hydrolysis sites of DPPC. It was concluded that hydrolysis at site A_1 causes the chiral transformation in the L-DPPC monolayer.

dx.doi.org/10.1021/jp2110314 | J. Phys. Chem. C 2012, 116, 14863−14872

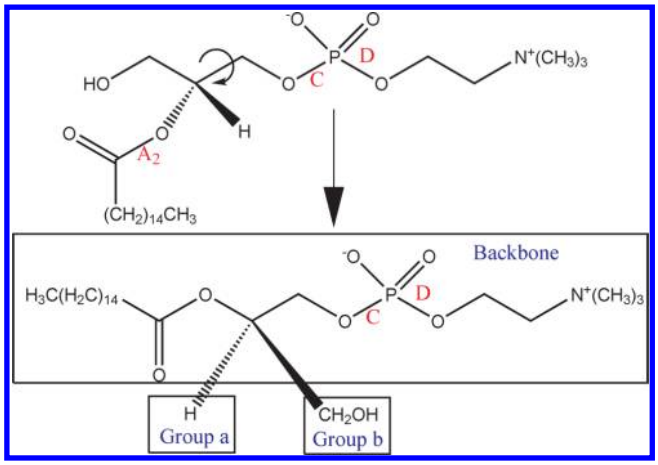

Figure 12. Structure of the hydrolyzate formed by hydrolysis at site A_1, which is contained in the backbone of L-DPPC. After hydrolysis at site A_1, the headgroup and group b make up the new backbone. The other part of the hydrolyzed chain turns into the new group b. Groups a and b of amphiphile A_1 are located opposite to where they are in L-DPPC with respect to the chiral center. Therefore, the twist direction between a pair of amphiphile A_1 is opposite to that between a pair of L-DPPC molecules.

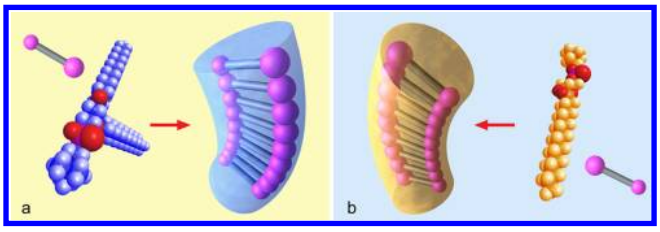

Figure 13. Helices formed by L-DPPC molecules (left) and the hydrolyzates formed by hydrolysis at site A_1 (right). The smaller pink ball represents group a and the larger pink ball represents group b. The helical directions of these two helices are opposite, as are their chiral states.

These results provide insight into the dynamics of lipid monolayer and bilayers and show that the chiral state of the domains in lipid monolayers varies with time. The results also indicate that the local environment has an effect on the interactions between lipid molecules and therefore should be taken into account, especially for complex biological systems. One may in future investigate other similar lipid systems through the use of the methods presented in this work and the use of sum-frequency-generation vibrational spectroscopy (SFG-VS), which is an alternative method because of its sensitivity to both interfaces and functional groups.

AUTHOR INFORMATION

Corresponding Author

*E-mail: guoyuan@iccas.ac.cn.

Notes

The authors declare no competing financial interest.

ACKNOWLEDGMENTS

We thank Prof. Hong-Fei Wang for suggestions and Prof. Mao-Xia for quantum calculations. Y.G. thanks funding from Natural Science Foundation of China (NSFC no. 91027042, no. 21073199) and the Ministry of Science and technology of China (MOST no. 2007CB815205).

REFERENCES

(1) Nag, K. *Structure and Dynamics of Membranous Interfaces*; Wiley: New York, 2008.
(2) Seul, M.; Andelman, D. *Science* **1995**, *267*, 476−483.
(3) Mcconnell, H. M. *Annu. Rev. Phys. Chem.* **1991**, *42*, 171−195.
(4) Simpson, G. J. *ChemPhysChem* **2004**, *5*, 1301−1310.
(5) Haupert, L. M.; Simpson, G. J. *Annu. Rev. Phys. Chem.* **2009**, *60*, 345−365.
(6) Houslay, M. D.; Stanley, K. K. *Dynamics of Biological Membranes*; Wiley: New York, 1982.
(7) Kulakowska, A.; Jurkiewicz, P.; Sykora, J.; Benda, A.; Mely, Y.; Hof, M. J. *Fluorescence* **2010**, *20*, 563−569.
(8) John, K.; Schreiber, S.; Kubelt, J.; Herrmann, A.; Muller, P. *Biophys. J.* **2002**, *83*, 3315−3323.
(9) Liu, J.; Conboy, J. C. *Vib. Spectrosc.* **2009**, *50*, 106−115.
(10) Anglin, T. C.; Conboy, J. C. *Biochemistry* **2009**, *48*, 10220−10234.
(11) Anglin, T. C.; Brown, K. L.; Conboy, J. C. *J. Struct. Biol.* **2009**, *168*, 37−52.
(12) Anglin, T. C.; Cooper, M. P.; Li, H.; Chandler, K.; Conboy, J. C. *J. Phys. Chem. B* **2010**, *114*, 1903−1914.
(13) Liu, J.; Conboy, J. C. J. *Phys. Chem. C* **2007**, *111*, 8988−8999.
(14) Anglin, T. C.; Conboy, J. C. *Biophys. J.* **2008**, *95*, 186−193.
(15) Liu, J.; Conboy, J. C. *Biophys. J.* **2005**, *89*, 2522−2532.
(16) Mcconnell, H. M.; Tamm, L. K.; Weis, R. M. *Proc. Natl. Acad. Sci. U. S. A.* **1984**, *81*, 3249−3253.
(17) Kruger, P.; Losche, M. *Phys. Rev. E* **2000**, *62*, 7031−7043.
(18) Ou-yang, W.; Yamamoto, T.; Aida, T.; Manaka, T.; Iwamoto, M. *Thin Solid Films* **2008**, *516*, 2649−2651.
(19) Nandi, N.; Vollhardt, D. *Chem. Rev.* **2003**, *103*, 4033−4076.
(20) Shen, Y. R. *Annu. Rev. Phys. Chem.* **1989**, *40*, 327−350.
(21) Shen, Y. R. *Nature* **1989**, *337*, 519−525.
(22) Verbiest, T.; Kauranen, M.; Maki, J. J.; Teerenstra, M. N.; Schouten, A. J.; Nolte, R. J. M.; Persoons, A. *J. Chem. Phys.* **1995**, *103*, 8296−8298.
(23) Xu, Y. Y.; Rao, Y.; Zheng, D. S.; Guo, Y.; Liu, M. H.; Wang, H. F. *J. Phys. Chem. C* **2009**, *113*, 4088−4098.
(24) Xu, Y. Y.; Wei, F.; Wang, H. F. *J. Phys. Chem. C* **2009**, *113*, 4222−4226.
(25) Lai, C. C.; Yang, S. H.; Finlaysonpitts, B. J. *Langmuir* **1994**, *10*, 4637−4644.
(26) Wadia, Y.; Tobias, D. J.; Stafford, R.; Finlayson-Pitts, B. J. *Langmuir* **2000**, *16*, 9321−9330.
(27) Thompson, K. C.; Rennie, A. R.; King, M. D.; Hardman, S. J. O.; Lucas, C. O. M.; Pfrang, C.; Hughes, B. R.; Hughes, A. V. *Langmuir* **2010**, *26*, 17295−17303.
(28) Liljeblad, J. F. D.; Bulone, V.; Tyrode, E.; Rutland, M. W.; Johnson, C. M. *Biophys. J.* **2010**, *98*, L50−L52.
(29) Zuidam, N. J.; Crommelin, D. J. A. *Int. J. Pharm.* **1995**, *126*, 209−217.
(30) He, Q.; Li, J. B. *Adv. Colloid Interface Sci.* **2007**, *131*, 91−98.
(31) Glendening, E. D.; Badenhoop, J. K.; Reed, A. E.; Carpenter, J. E.; Bohmann, J. A.; Morales, C. M.; Weinhol, F. *NBO 5.0*; NBO: Theoretical Chemistry Institute, University of Wisconsin: Madison, WI, 2001.
(32) Frisch, M. J.; Trucks, G. W.; Schlegel, H. B.; Scuseria, G. E.; Robb, M. A.; Cheeseman, J. R.; Montgomery, J. A., Jr.; Vreven, T.; Kudin, K. N.; Burant, J. C.; et al. *Gaussian 03*; Gaussian, Inc.: Pittsburgh, PA, 2003.
(33) Helfrich, W. *J. Chem. Phys.* **1986**, *85*, 1085−1087.
(34) Helfrich, W.; Prost, J. *Phys. Rev. A* **1988**, *38*, 3065−3068.
(35) Selinger, J. V.; Schnur, J. M. *Phys. Rev. Lett.* **1993**, *71*, 4091−4094.
(36) Ouyang, Z. C.; Liu, J. X. *Phys. Rev. Lett.* **1990**, *65*, 1679−1682.
(37) Zhongcan, O. Y.; Liu, J. X. *Phys. Rev. A* **1991**, *43*, 6826−6836.
(38) Servuss, R. M.; Harbich, W.; Helfrich, W. *Biochim. Biophys. Acta, Biomembr.* **1976**, *436*, 900−903.
(39) Nandi, N.; Bagchi, B. *J. Am. Chem. Soc.* **1996**, *118*, 11208−11216.

(40) Nandi, N.; Bagchi, B. *J. Phys. Chem. A* **1997**, *101*, 1343−1351.
(41) Nandi, N.; Vollhardt, D. *J. Phys. Chem. B* **2003**, *107*, 3464−3475.
(42) Bondi, A. *J. Phys. Chem.* **1964**, *68*, 441−451.
(43) Benamotz, D.; Herschbach, D. R. *J. Phys. Chem.* **1990**, *94*, 1038−1047.